This article has been accepted for publication in a future issue of this journal, but has not been fully edited. Content may change prior to final publication. Citation information: DOI 10.1109/TIA.2020.3029547, IEEE Transactions on Industry Applications

AFF-SOGI-DRC Control of Renewable Energy Based Grid Interactive Charging Station for EV with Power Quality Improvement

Anjeet Verma, *Member, IEEE* and Bhim Singh, *Fellow, IEEE*

***Abstract*— In this paper, a control of solar photovoltaic (PV) array, and wind energy conversion system (WECS) based charging station using an adaptive frequency fixed second order generalized integrator with DC offset rejection capability (AFF-SOGI-DRC), is presented for charging the electric vehicle (EVs) and improving the power quality of the grid. In comparison to SOGI-based algorithm, wherein a frequency feedback loop reduces the stability margin and FF-SOGI-based algorithm, where a double frequency oscillation and offset error constraint the algorithm capability, the presented algorithm precisely estimates the fundamental EV current. Moreover, the AFF-SOGI-DRC based positive sequence extractor helps in generating the sinusoidal in-quadrature unit vectors under distorted and unbalanced grid voltages; therefore, the reference grid currents become harmonic free. The charging station is operated in the grid connected mode (GCM) and an islanded mode (IM) to utilize the renewable energy maximally. The control of the charging station also includes the voltage synchronizing strategy that ensures the smooth transition between the GCM and IM. Moreover, a unified controller is designed to achieve four-quadrant operation (V2G/G2V), vehicle to home power transfer, reactive power compensation and active filtering etc. The operation of the charging station complies with the IEEE 1547 standard, and the operation of the charging station is validated through the laboratory prototype.**

***Keywords*— Electric vehicle (EV), solar PV generation, wind energy conversion, bi-directional power flow, power quality.**

I. INTRODUCTION

Currently, the electric vehicles (EVs) are considered as the alternative to the internal combustion engine based vehicles due to clean, emission less, and environment friendly transportation [1]-[2]. However, massive charging infrastructure is required to meet the charging demand of EVs, which is mostly supported by the grid [3]. Due of which, many grid-related problems such as voltage sag, swell, distortions, unbalance, current distortions, DC offset in current etc. [4] are frequently appearing. Therefore, it is very much important to design a system, which can charge EVs and improves the power quality of the grid, simultaneously [5]. Control algorithms are effective tool to mitigate the power quality problems. Therefore, in this paper, an adaptive frequency-fixed-second order generalized integrator with DC offset rejection capability (AFF-SOGI-DRC) based algorithm is utilized to control the charging station and to enhance the grid's power quality under distorted and unbalance voltages conditions with the presence of DC offset in the load currents. In the literature, many algorithms have been used to improve the power quality at the grid. Instantaneous reactive power theory (IRPT) [6] and synchronous reference frame theory (SRFT) [7] are most popular and widely used algorithms in the grid connected applications. IRPT algorithm converts the three phase voltage and currents to two phase voltage and currents for calculating the active and reactive power of the load. Moreover, due to the use of a low pass filter and a PI controller for DC voltage regulation used for output power calculation, the transient response of the IRPT algorithm is relatively poor. Moreover, the IRPT performance deteriorates at distorted and unbalanced grid voltages. Similarly, the effectiveness of SRFT algorithm is also severely affected by the efficacy of the PLL at unbalanced and distorted voltages. Enhanced PLL (EPLL) [8] based algorithm demonstrates the excellent tracking efficiency at unbalanced and distorted voltages. However, due to the use of a trigonometric function, EPLL algorithm becomes computationally expensive. Second order generalized integrator (SOGI) [9] based algorithm offers good tracking capability, fast convergence and low steady state error. However, at variable frequency, performance of SOGI algorithm also deteriorates. Therefore, a frequency feedback loop is suggested in the literature to make the SOGI algorithm frequency adaptive but at the cost of increased computation and reduced stability margin. Moreover, the frequency-dependent tuning makes it difficult for implementation. The notch filters [10] offer performance similar to SOGI algorithms. However, the selection of centre frequency of a notch filter at variable frequency becomes cumbersome, which affects performance of the NF. Therefore, some adaptive notch filters (ANF) [11] are also proposed in the literature for changing the centre frequency as the signal frequency changes. However, again the frequency feedback loop restricts the performance of ANF. SOGI-frequency locked loop (SOGI-FLL) [12] solves the problem of frequency feedback and offers superior performance than SOGI and other algorithms. However, the input signal amplitude-dependent tuning of frequency update law in SOGI-FLL, makes it difficult to implement at variable voltage condition. In the literature, many attempts have been made to remove the frequency feedback loop and use frequency-fixed SOGI (FF-SOGI) [13] to improve its performance. However, the FF-SOGI algorithm generates an in-quadrature signal of unequal magnitude other than nominal frequency. Therefore, to generate in-quadrature signal of equal magnitude, Xiao et al. [14] have proposed to multiply the quadrature signal with a gain equal to the ratio of frequency drift and the nominal frequency. However, due to the use of SRF-PLL for frequency estimation, the FF-SOGI algorithm becomes computationally expensive. Further, adaptive FF-SOGI (AFF-SOGI) algorithm is proposed by Akhtar et al. [15] for completely removing the frequency estimation and making the FF-SOGI truly adaptive to the frequency variation for achieving the in-quadrature voltages of equal amplitude. Though, the AFF-SOGI algorithm poses all characteristics of SOGI algorithm and generates in-quadrature voltages of equal magnitude at distorted and unbalanced voltages and frequency variation too, however, performance of AFF-SOGI deteriorates at presence of DC offset in input signal and fundamental-frequency oscillatory errors appear in estimated phase, frequency, and amplitude. Therefore, in this

work, AFF-SOGI-DRC is presented to control charging station and to improve the power quality of the grid.

EV charging generally obtains power from conventional sources of energy that utilizes fossil fuels. Therefore, the use of electricity generated by fossil fuels does not eliminate the emission but merely moves it from vehicles to power plant. Thus, the EVs powered by the energy generated from the green energy sources (solar and wind etc.), can be a true alternative of IC engine based vehicles for the elimination of emission and providing environmental advantage [16]-[20]. Mouli et al. [21] have presented a high power EV charger for utilization of solar PV array energy. Alharbi et al. [22], and Verma et al. [23] have suggested the PV array integrated EV charger for self-sustained, reliable, clean and cost-effective charging. Li et al. [24] have proposed a fast charging facility using a solar PV array, wind energy and a storage battery based distributed energy sources. Therefore, in this paper, the PV array and wind energy conversion system (WECS) are used for EV charging.

The most common way to integrate the PV array with the charging station is through a DC-DC boost converter, which is used for maximum power point tracking of PV array [25]-[28]. However, in this paper, the DC-DC conversion stage is eliminated, and a PV array is directly interfaced to charging station using a diode. The key benefit of this topology involves a power stage reduction, by a removal of boost converter, without sacrificing the efficacy of a PV array. Besides, the topology provided is a kind of retrofit approach in which the PV array can be added to the current charging network with minimal software modification (MPPT algorithm) alone.

Similarly, in this paper, instead of using a VSC for the integration of a permanent magnet brushless DC generator (PMBLDCG), a simple topology consisting only of a diode bridge rectifier followed by a boost converter is used for the conversion of power from WECS based on PMBLDCG. The major motivation behind the choice of this topology is to the quasi square wave nature of the PMBLDCG currents, which match with the input currents of the rectifier. Hence, the performance of the PMBLDCG is not affected by the quasi square wave current of the rectifier, which is not the condition with machines with sinusoidal currents such as PMSG and DFIG based WECS. Another major advantage of this topology, is that the maximum power is extracted using a boost converter using only rectifier output voltage and current. Moreover, this topology also does not require wind speed information and turbine characteristics for MPPT. As compared to VSC based WECS [29], [30], this topology reduces circuit complexity, size of power converter cost, without sacrificing WECS power generation. Moreover, it is also easy to implement.

Therefore, this paper deals with a PV array and WECS based multifunctional charging station for power quality improvement at the grid using AFF-SOGI-DRC. Followings are main objectives of this work.

- Design of a PV array and WECS based integrated system for EV charging and household supply.
- An AFF-SOGI-DRC based control algorithm is used to control the charging station and to enhance the grid's power quality at distorted and unbalance voltages with the presence of DC offset in load currents.
- A PV array and WECS are connected to the charging station using a simple architecture for reducing the size of the converter without affecting the performance.
- To utilize the quasi square wave nature of PMBLDCG currents, the rectifier and boost converter based topology is used. Moreover, the PV array is connected to the charging station without a boost converter.
- To increase the operational efficiency of the charging station, the operation of charging station is presented in an islanded mode (IM), and grid connected mode (GCM). Moreover, a unified controller is designed to achieve four-quadrant operation (V2G/G2V), vehicle to home power transfer, reactive power compensation and active filtering.
- In addition, charging station has a capability to change the mode, i.e. IM to GCM and vice versa, so that charging remains continuous irrespective of grid availability and the solar and wind disturbances.

II. System Configuration and Control Algorithm

The presented integrated charging station, as shown in Fig. 1, interfaces the PV array and WECS using VSC for the purpose of providing the charging facility to the EV and supplying power to domestic loads in both IM and GCM. The PV array is interfaced to the DC link of the charging station. However, the PMBLDC generator based wind energy conversion system (WECS) is coupled to the DC link through a diode bridge rectifier followed by a boost converter. The purpose of the boost converter is to harness the peak power of WECS. The EV takes power from the point of common coupling (PCC) and DC link of the charging station using a bi-directional DC-DC converter (BDC). The domestic loads are coupled at PCC of the system. A bidirectional static switch and interfacing inductors are used between PCC of the charging station and the grid. Moreover, the RC filters are also used to remove the switching harmonics.

The purpose of charging station is to provide an uninterruptible charging to EVs in all operating conditions and backup power to the household loads in case of emergency. Therefore, the control of charging station is designed to provide the services in both IM and GCM. Moreover, the controller has to enhance the grid's power quality and to make sure that the charging station operation remains undisturbed at unbalanced and polluted grid voltages. Besides, the controller has to extract the maximum power from renewable sources. Based on the objective of the charging station, the control is designed for GCM, IM, MPPT of WECS and scheme for storage battery charging. Fig. 2 shows a combined control strategy of the charging station.

A. VSC Control in GCM

The GCM control is designed with the objectives of improving the power quality at the grid by harmonics mitigation and compensating the reactive power demand of household and EV loads. Moreover, balancing the grid currents and making them pure sinusoid at distorted and unbalanced voltages, is also an objective. Therefore, the grid connected control estimates the sinusoidal reference grid currents using the AFF-SOGI-DRC, irrespective of distorted load currents, EV currents and distorted grid voltages.

The AFF-SOGI-DRC algorithm considers only the fundamental frequency currents. It rejects the other frequency component for generating the reference currents so that the other frequency component currents do not flow into the grid and only active power is taken from the grid. In addition, the controller uses the unit voltage vectors estimated from the positive sequence voltages of the grid so that the distortions and unbalance in the grid voltages do not affect the reference currents. The detailed control scheme for grid connected mode is shown in Fig. 2. Here, AFF-SOGI-DRC is used for fundamental current

This article has been accepted for publication in a future issue of this journal, but has not been fully edited. Content may change prior to final publication. Citation information: DOI 10.1109/TIA.2020.3029547, IEEE Transactions on Industry Applications

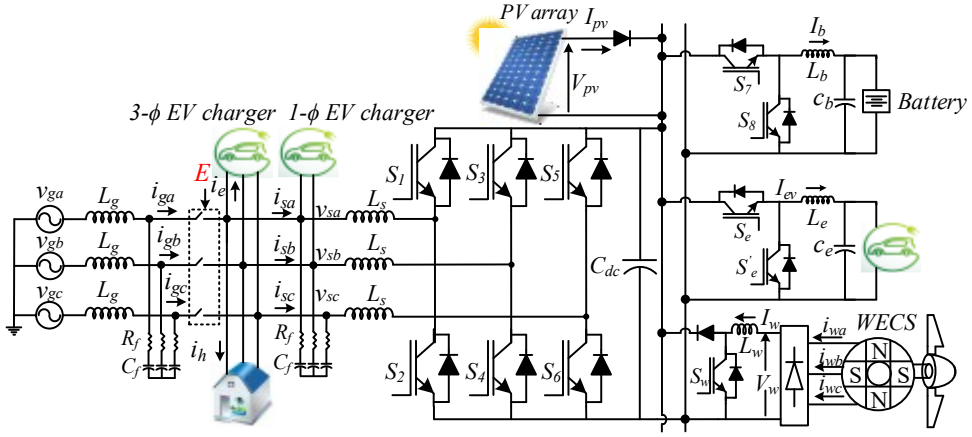

Fig. 1 Configuration of charging station

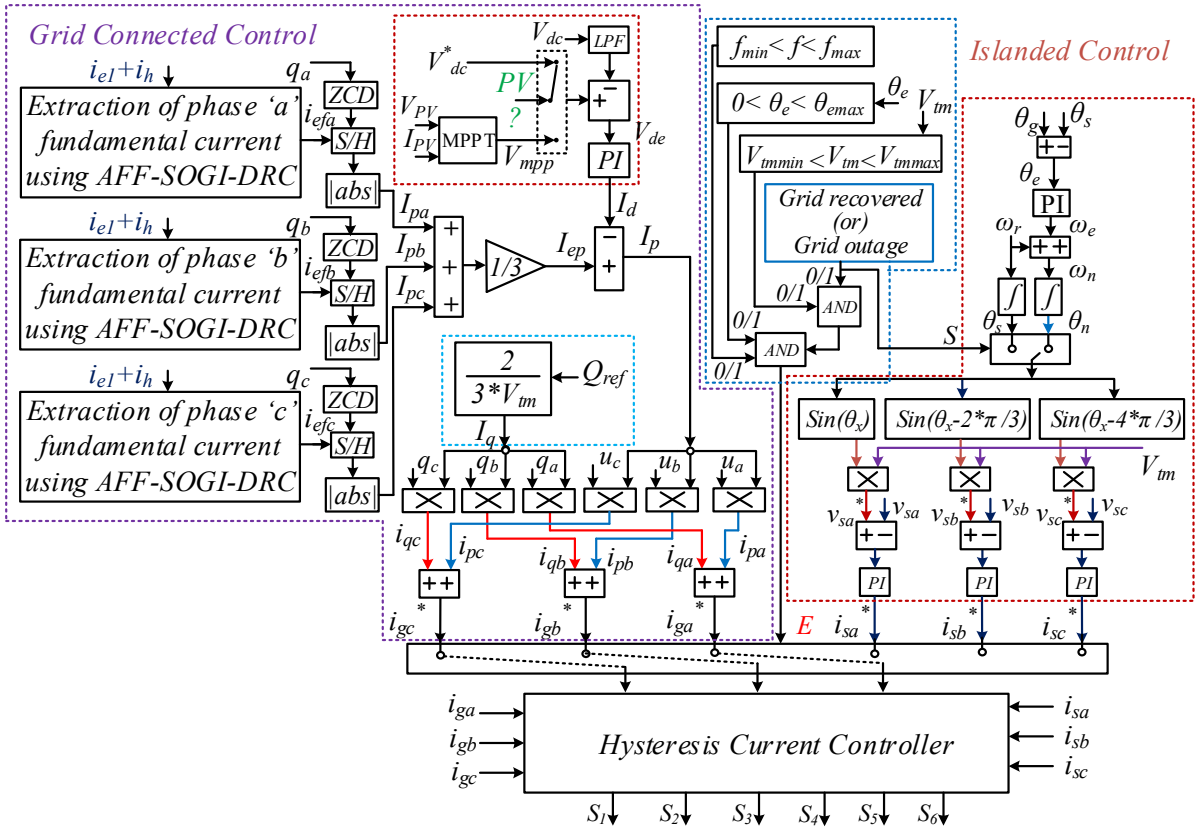

Fig. 2 Combined control strategy of charging station for both islanded and grid connected mode

extraction, which is derived from the FF-SOGI algorithm by replacing the damping factor and resonant frequency with the fractional order damping factor and fractional order resonant frequency. Moreover, a DC offset rejection loop is added to the AFF-SOGI so that fundamental current estimation becomes immune to the DC offset present in the EV current. The block diagram of AFF-SOGI-DRC is shown in Fig. 3.

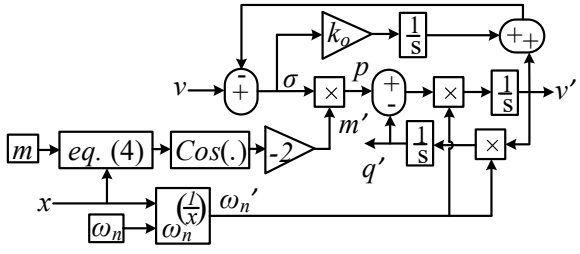

Fig. 3 Control diagram of AFF-SOGI-DRC

The in-quadrature transfer function of AFF-SOGI-DRC is as,

$$\frac{v'}{v}=\frac{m'\omega_n's^2}{s^3+(k_o+m'\omega_n')s^2+(\omega_n')^2s+k_o(\omega_n')^2} \quad (1)$$

$$\frac{q'}{v}=\frac{m'(\omega_n')^2s}{s^3+(k_o+m'\omega_n')s^2+(\omega_n')^2s+k_o(\omega_n')^2} \quad (2)$$

where v' and q' are in-quadrature signals of the fundamental frequency. m' and ω_n' are fractional order damping factor and fractional order resonant frequency which is defined as,

$$m'=-2\cos(\mu/x), \quad \omega_n'=\omega_n^{1/x} \quad (3)$$

Where $\omega_n=2\pi f$ rad/s and m is a constant whose value is selected on the basis of settling time and overshoot during transient of AFF-SOGI. In (4), the ratio μ/x is defined as,

This article has been accepted for publication in a future issue of this journal, but has not been fully edited. Content may change prior to final publication. Citation information: DOI 10.1109/TIA.2020.3029547, IEEE Transactions on Industry Applications

$$\mu/x=\begin{cases}\pi-\tan^{-1}\dfrac{\sqrt{4-m^2}}{m} & 0<m<2\\ \pi & m\geq 2\end{cases} \tag{4}$$

The AFF-SOGI-DRC is derived from FF-SOGI; therefore, it is tuned for fixed value of the m and ω_n. However, AFF-SOGI-DRC is made adaptive to grid frequency variations by changing m' and ω_n' using x. Here, the transfer function is shown for estimation of in-quadrature voltages. However, the algorithm is equally valid for estimating fundamental load + EVs currents.

After the estimation of fundamental currents, the active current is estimated by sampling the fundamental current at every zero crossings of quadrature unit vectors and holding it up to the next zero crossings. For identifying the zero crossing, a zero crossing detector (ZCD) is used. Unit vectors carry phase and frequency of grid voltages, which are used for synchronization. Therefore, unit vectors should be a pure sinusoid of unit amplitude even at distorted and unbalanced voltages. For this purpose, the positive sequence voltages are used for the unit vectors generations. The grid positive sequence voltages are obtained from the double AFF-SOGI-DRC as exhibited in Fig. 4.

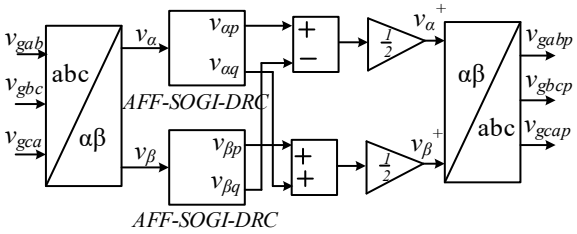

Fig. 4 Positive sequence estimation using double AFF-SOGI-DRC

Now, the phase voltages of the grid are estimated as,

$$v_{ga}=\frac{1}{3}\left(2v_{gabp}+v_{gbcp}\right), v_{gb}=\frac{1}{3}\left(-v_{gabp}+v_{gbcp}\right)$$
$$v_{gc}=\frac{1}{3}\left(-v_{gabp}-2v_{gbcp}\right) \tag{5}$$

Where, v_{gabp}, v_{gbcp} and v_{gcap} are positive sequence line voltages of grid and v_{ga}, v_{gb} and v_{gc} are the phase voltages of grid. Whereas, v_{gab}, v_{gbc} and v_{gca} are line voltages of the grid.

The amplitude of PCC voltages, V_{tm}, in-phase (u_a, u_b, u_c) and quadrature-phase (q_a, q_b, q_c) unit templates are estimated as,

$$V_{tm}=\sqrt{\frac{2}{3}\left(v_{ga}^2+v_{gb}^2+v_{gc}^2\right)} \tag{6}$$

$$u_a=\frac{v_{ga}}{V_{tm}}, u_b=\frac{v_{gb}}{V_{tm}}, u_c=\frac{v_{gc}}{V_{tm}} \tag{7}$$

$$q_a=-\frac{u_a}{\sqrt{3}}+\frac{u_c}{\sqrt{3}},\ q_b=\frac{\sqrt{3}u_a}{2}+\frac{(u_b-u_c)}{2\sqrt{3}}$$
$$q_c=-\frac{\sqrt{3}u_a}{2}+\frac{(u_b-u_c)}{2\sqrt{3}} \tag{8}$$

With active currents of three phases, its average active current is calculated as,

$$I_{ep}=\frac{I_{pa}+I_{pb}+I_{pc}}{3} \tag{9}$$

Due to the average active currents, the cumulative requirement of the load + EV, is equally distributed in three phases. As a result, the grid currents always remain balanced irrespective of the unbalanced voltages and unequal load demand.

The total active current of reference grid current is calculated as,

$$I_p=I_{ep}-I_d \tag{10}$$

In (10), I_d is the current required for regulating the DC link voltage, is obtained as,

$$I_d(r)=I_d(r-1)+k_{pd}\{V_{de}(r)-V_{de}(r-1)\}+k_{id}V_{de}(r) \tag{11}$$

Where V_{de} is an error between the reference DC link voltage and sensed DC link voltage. k_{pd}, and k_{id} are the proportional and integral gains of PI controller, respectively.

Here, the PV array is feeding power to the DC link; therefore, in GCM, the MPPT is achieved by maintaining the DC link voltage at MPP voltage using VSC. Whereas, in IM, MPPT is achieved by BDC of the battery. In both operating modes, the DC link reference voltage is obtained from the incremental conductance (INC) MPPT algorithm. However, the DC link voltage is controlled at 400V in absolute lack of PV array power, as shown in Fig. 2.

The reactive current of the reference grid is obtained as,

$$I_q=\frac{2Q_{ref}}{3V_{tm}} \tag{12}$$

Here, Q_{ref} is the user given command for the vehicle to grid reactive power compensation.

Now, using (7), (8), (10) and (12), the sinusoidal active and reactive reference grid currents are estimated as,

$$i_{pa}=I_p*u_a,\ i_{pb}=I_p*u_b,\ i_{pc}=I_p*u_c \tag{13}$$

$$i_{qa}=I_q*q_a,\ i_{qb}=I_q*q_b,\ i_{qc}=I_q*q_c \tag{14}$$

Finally, the reference currents for the grid are obtained as,

$$i_{ga}^*=i_{pa}+i_{qa},\ i_{gb}^*=i_{pb}+i_{qb},\ i_{gc}^*=i_{pc}+i_{qc} \tag{15}$$

Fig. 5 shows the fundamental current estimation, active current and the reference current estimation performance of the AFF-SOGI-DRC based control algorithm.

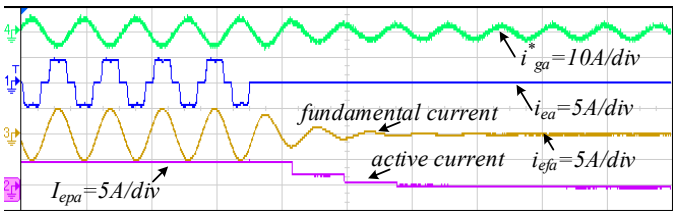

Fig. 5 Fundamental current, active current and grid reference current generation

B. VSC Control in Islanded Mode and Control for Seamless Mode Change (IM ↔ GCM)

The IM control is designed to use WECS and PV array power and to operate the charging station at unavailability of the grid. Therefore, AC voltages are generated at PCC according to the control exhibited in Fig. 2. This control generates sinusoidal reference voltages (v_{sa}^*, v_{sb}^*, v_{sc}^*). Comparing reference voltages (v_{sa}^*, v_{sb}^*, v_{sc}^*) with sensed voltages, and minimizing the voltage errors using PI regulators generate the current references for PCC. The reference currents and sensed PCC currents generate the gate signals for insulated gate bipolar junction transistors (IGBTs) switches of VSC using a hysteresis controller.

The IM control also discusses the logic for seamless mode transition from an IM to the GCM and vice. For this, the controller always samples the grid and the PCC voltages and monitors the phase error between these two voltages and decides the mode of operation. For changing the mode from an IM to the GCM, the phase error is initially determined, and a PI controller minimizes the error in phase and expresses the error in terms of frequency error. The frequency error is calculated as,

$$\omega_e(r)=\omega_e(r\text{-}1)+k_{pa}\left\{\theta_e(r)\text{-}\theta_e(r\text{-}1)\right\}+k_{ia}\theta_e(r) \tag{16}$$

This article has been accepted for publication in a future issue of this journal, but has not been fully edited. Content may change prior to final publication. Citation information: DOI 10.1109/TIA.2020.3029547, IEEE Transactions on Industry Applications

Where θ_e is phase error and k_{pa} and k_{ia} are the controller gains. Using (16), the updated frequency is calculated as,

$$\omega_n = \omega_r + \omega_e \tag{17}$$

The converter generates the voltage of updated frequency as long as the phase error does not match the conditions shown in Fig. 2. When all the conditions are satisfied, the controller enables the signal 'E' for connecting the PCC to the grid.

C. Bi-directional Converter Control for Storage Battery

In GCM, the battery is operated in grid to storage (G2S) and storage to grid (S2G). In G2S mode, a constant current and constant voltage (CC/CV) strategy is used, as shown in Fig. 6. However, in S2G mode, the battery is discharged in constant current/power mode. This value of current/power depends on a commitment of charging station to the utility. The PI controller used in the outer voltage loop for battery voltage regulation and estimation of battery reference current is obtained as,

$$I_b^*(r) = I_b^*(r-1) + k_{ps}\{V_{be}(r) - V_{be}(r-1)\} + k_{is}V_{be}(r) \tag{18}$$

Where V_{be} is the error in the battery voltage and the k_{ps}, k_{is} are the regulator gains.

The inner current loop used for the estimation of duty ratio is determined as,

$$d_e(r) = d_e(r-1) + k_{pb}\{I_{be}(r) - I_{be}(r-1)\} + k_{ib}I_{be}(r) \tag{19}$$

Where I_{be} is an error in the battery current and k_{pb}, k_{ib} are controller gains.

Using the duty ratio, a pulse width modulator (PWM) gives the switching pulses for the converter.

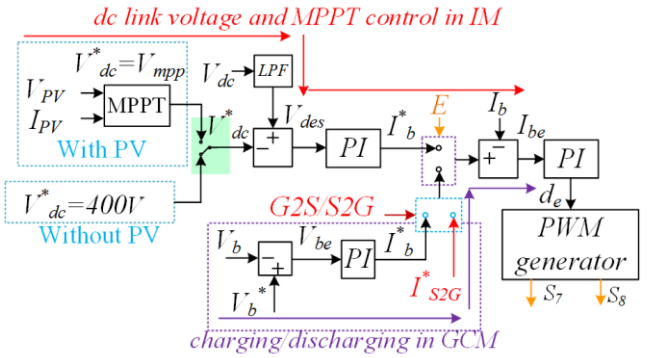

Fig. 6 Control of BDC of the storage battery

In IM, the DC link voltage is regulated by the storage battery using the bidirectional DC-DC converter. Moreover, the MPPT of the PV array is also achieved using a bi-directional converter. Therefore, the DC link reference voltage is selected based on the availability of PV array, as discussed in III.A. Here, the PI voltage regulator gives the battery reference current using which the current controller in (19), gives the duty ratio and the switching pulses are obtained from the PWM generator.

D. MPPT Control of WECS

The MPPT control of WECS is achieved using a scheme shown in Fig. 7. For MPPT, the voltage and current of the rectifier output are given to an INC MPPT algorithm, and it estimates the voltage corresponding to the maximum power. Further, the triggering signals for a boost converter are obtained from the PWM generator using the MPP voltage and the DC link voltage.

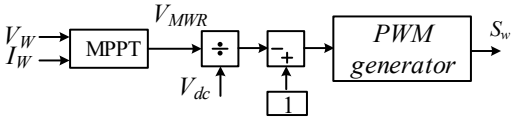

Fig. 7 MPPT scheme for the WECS

III. Results And Discussion

An experimental prototype of the charging station developed in the laboratory, is shown in Fig. 8. The operating capability of the system is presented in both dynamic conditions and steady state operating conditions (Figs. 9-16). This system operates in both GCM and IM conditions, and the dynamic performances are shown in both IM and GCM. For experimental validation, a solar PV array of 2.5kW, 460V, and 9.5A is used. The rating of PMBLDCG based WECS system is 2 kW. The rating of a battery is 240 V and 35 Ah. The control algorithm of the system is implemented in a digital controller dSPACE (1006) utilizing current and voltage signals acquired using voltage transducers (LEM LV-25P) and current transducers (LEM LA-55P).

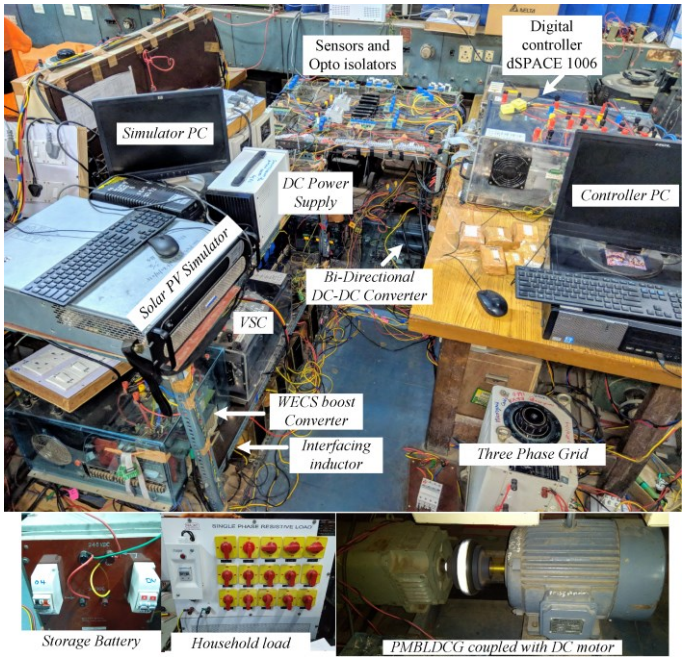

Fig. 8 Experimental prototype of charging station

A. Steady State Results

The steady state results of the system in GCM, are shown in Fig. 9. Together, a solar PV array (Fig. 9(g)) and WECS (Figs. 9(c)-(d)) are generating 5.5kW. A power of 1.7 kW is taken by the home load (Figs. 9(e)-(f)), 1.08 kW is taken by the battery (Fig. 9(h)) and remaining 2.5kW is fed into the grid at unity power factor (Figs. 9(a)-(b)). Fig. 9 (b) shows the grid current THD, which is less than 5%, even though the current drawn by the EVs connected at PCC is more than 20% as exhibited in Fig. 9(f). This signifies that VSC of the charging station is not only extracting maximum power from a solar PV array, but it is also compensating the nonlinearity of the EV current.

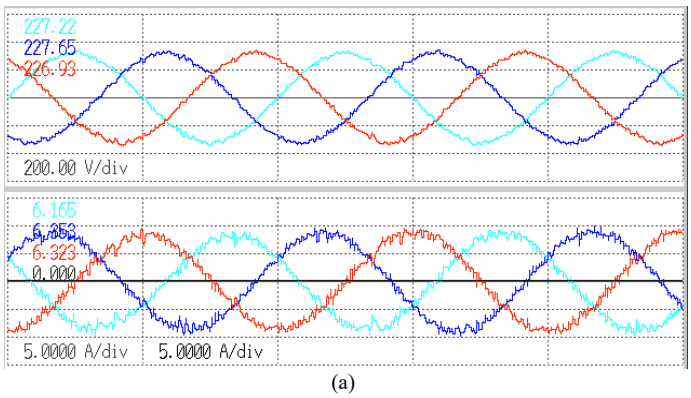

(a)

This article has been accepted for publication in a future issue of this journal, but has not been fully edited. Content may change prior to final publication. Citation information: DOI 10.1109/TIA.2020.3029547, IEEE Transactions on Industry Applications

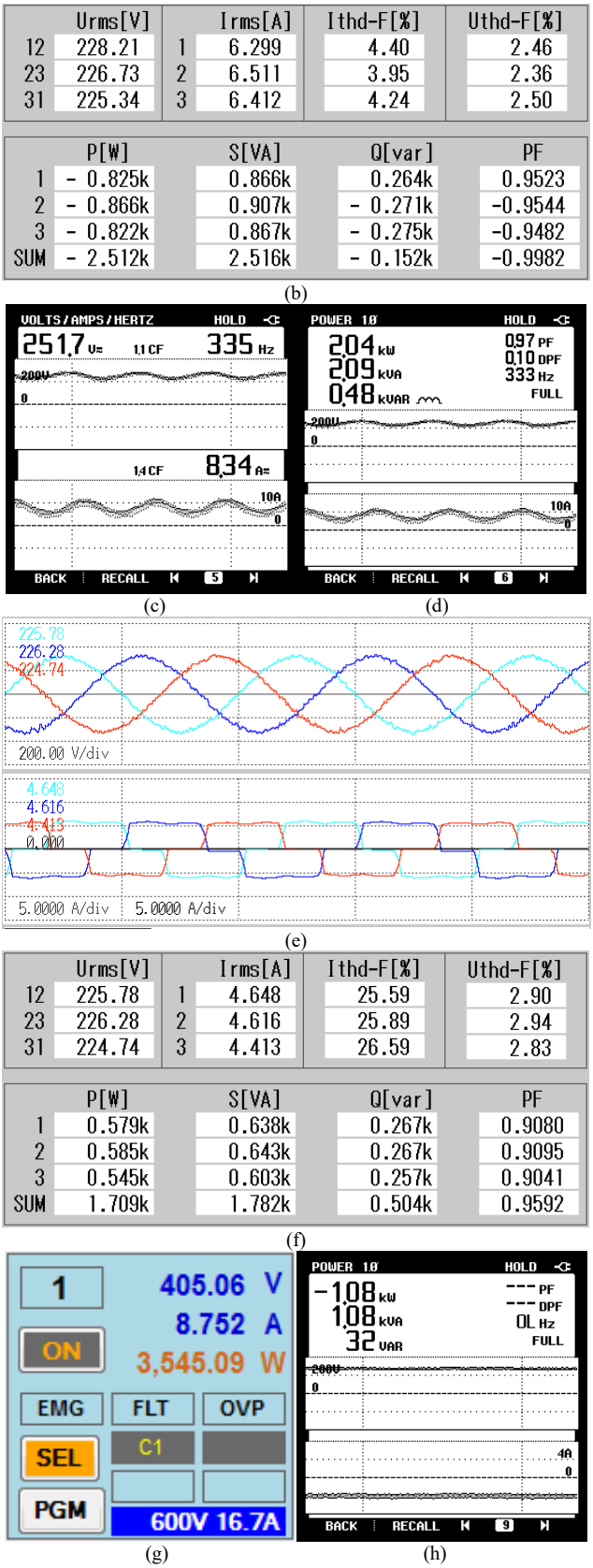

Fig. 9 Steady state response, (a) v_{ab}, v_{bc}, v_{ca} and i_{ga}, i_{gb}, i_{gc}, (b) active, reactive power of grid, THDs of v_{ab}, v_{bc}, v_{ca} and i_{ga}, i_{gb}, i_{gc}, (c)Vw and Iw, power PMBLDCG, (e) v_{ab}, v_{bc}, v_{ca} and i_h, (f) active, reactive power of home load, THDs of v_{ab}, v_{bc}, v_{ca} and i_h, (g) V_{pv}, I_{pv} and P_{pv}, (h) P_b

B. *Dynamic Performance*

The transient behavior of the system for the changes in solar irradiance, wind speed, and disturbance in the EV charging current, are shown in Figs. 10-11.

1) *Performance in Islanded Mode*

Fig. 10 shows the performance of the charging station in IM at solar irradiance and wind speed changes. Due to the perturbation in solar irradiance from 1000 W/m^2 to 500W/m^2, the solar PV array current decreases (Fig. 10(a)). Since the power of WECS and the power of the EV connected at PCC should not be disturbed, the battery starts discharging. Fig. 10(a) shows that WECS power and EV power are not getting affected due to the irradiance variation. Similarly, the change in wind speed causes a reduction in power generation (Fig. 10(b)). Therefore, the EV battery starts discharging to supply the load and the EV. Fig. 10(b) also shows the regulated DC link voltage and undisturbed sinusoidal PCC voltage. Therefore, it is observed that the disturbance due to one source is not affecting the generation of other source and EVs.

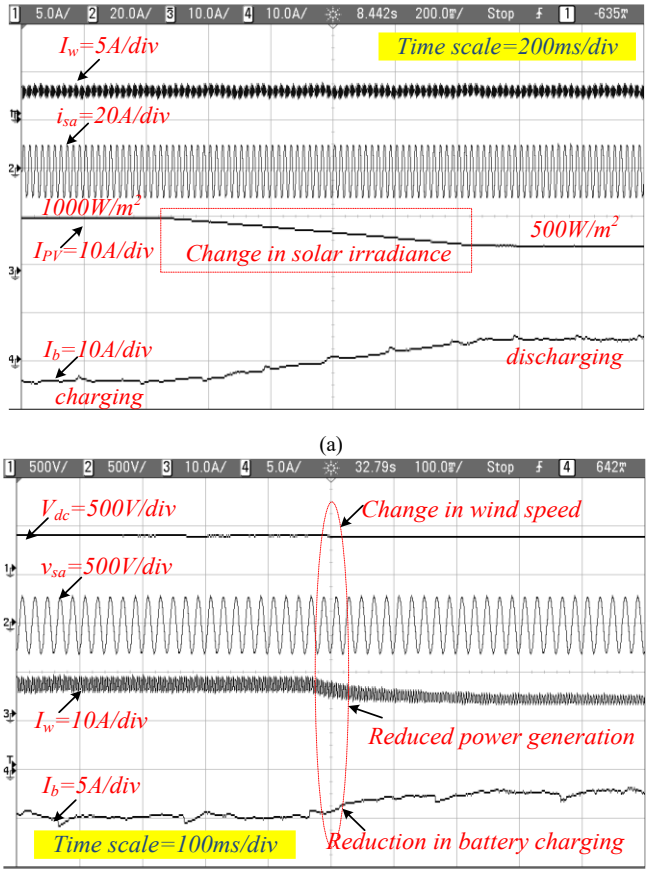

Fig. 10 Dynamic performance in standalone mode, (a) change in solar irradiance 1000W/m^2→500W/m^2, (b) change in wind speed

2) *Performance in Grid Connected Mode*

When connected to the grid, the battery current is changed in step from charging to discharging for showing the storage to grid capability of the charging station. The change in battery current causes an increase in the power supplied to the grid (Figs. 11(a)-(b)). However, the powers generated by the solar PV array and WECS are undisturbed. Moreover, the charging of EV connected at PCC is not getting disturbed, and the DC link voltage is also maintained. Similarly, the change in solar irradiance (Figs. 11(c)-(e)) and wind speed (Figs. 11(f)-(g)), only affects the grid power to maintain the power balance. Moreover, these transients don't affect the charging of EV battery, connected at PCC and DC link voltage. Similarly, the performance under the connection/disconnection of EV is shown in Fig. 11(h).

This article has been accepted for publication in a future issue of this journal, but has not been fully edited. Content may change prior to final publication. Citation information: DOI 10.1109/TIA.2020.3029547, IEEE Transactions on Industry Applications

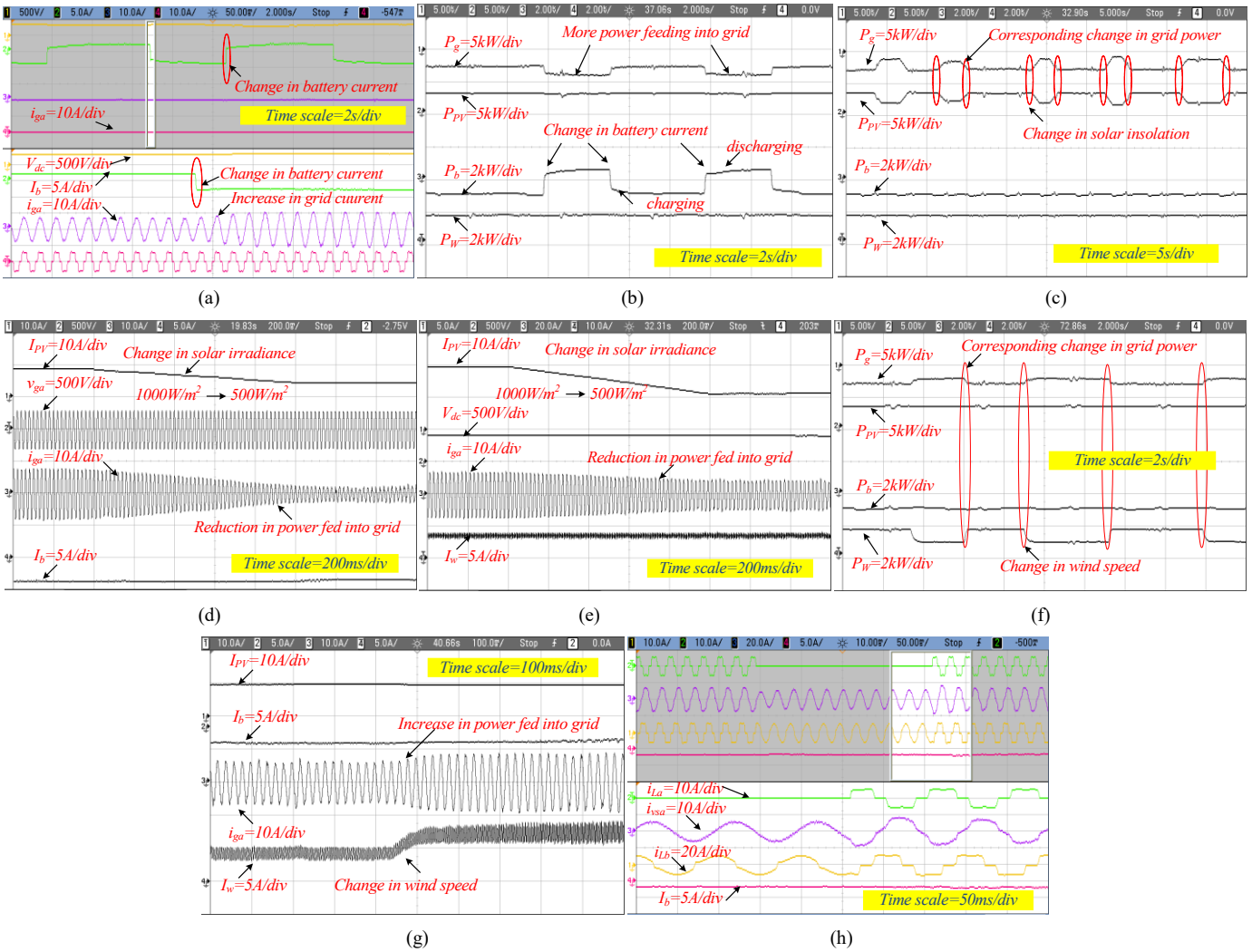

Fig.11 Dynamic performance in GCM, (a)-(b) change in EV current (I_B), (c)- (e) change in solar irradiance, (f)-(g) change in wind speed, (h) change in home load

The disconnection/connection of EV also does not affect the solar PV array power, WECS power, charging of EV and DC link voltage.

The charging station capability to operate at distorted and unbalanced voltages and to improve the quality of voltage and current are shown in Fig. 12. From Figs. 12(a)-(b), it is observed that after the compensation, the grid currents become balanced and sinusoidal. In addition, the grid voltage quality also improves as the current harmonics are not being fed into the grid after compensation. Fig. 12 (c) shows the current of VSC before and after compensation, which justifies that non-fundamental current of EV and household load is compensated by VSC.

Fig. 13 illustrates the synchronization of PCC voltage with the grid voltage for the seamless shift of operation for IM to GCM. From Fig. 13, it is observed that the charging station is connected to the grid only after the two voltages perfectly matches to each other. As a result, the transition happens to be very smooth, and grid current justifies it. Similarly, the shift of operation from GCM to IM is also smooth. It is also observed that during the mode change, the EV current is undisturbed.

Fig. 14 shows performance of charging station while supplying reactive power to the grid. From Fig. 14, it is observed that the reactive power command is changed in the step. As a result, the controller updates reference currents for supplying demanded power and the voltage and current justifies the same.

Fig. 15 shows a comparison of performance of AFF-SOGI-DRC with SOGI and AFF-SOGI algorithms, and it is observed that the fundamental current estimated by AFF-SOGI-DRC is sinusoidal whereas, other signals are not of good quality.

Fig. 16 shows the THD of grid current as a function of power fed into the grid in vehicle to grid mode. The graph is made using the readings taken on power quality analyzer (Fluke 43B). The minimum THD of the grid current is 1.4 % at 3kW, and the maximum THD is 4.8 % at 500W. Moreover, the power factor is unity for the entire power region.

IV. Conclusion

A PV array-WECS based multifunctional EV charging station has been controlled using AFF-SOGI-DRC. Test results have validated the controller ability to extract the fundamental currents from the polluted currents and estimated the distortion free and balanced grid reference currents under all operating conditions including unbalanced and distorted voltages. Test results also show that the THDs of grid voltage and current, are always maintained less than 5%, even for worst operating conditions. In addition, test results have validated the charging station capability to simultaneously charge the EV and to feed the household loads in both GCM and IM. In IM, the charging station has generated the sinusoidal voltages with good quality in terms of THD, irrespective of EV and home load currents. The controller has always extracted the peak power from the PV array, and WECS and the same have been justified by test results in dynamic conditions. Moreover, the power management capability of the charging station and its controller has been

This article has been accepted for publication in a future issue of this journal, but has not been fully edited. Content may change prior to final publication. Citation information: DOI 10.1109/TIA.2020.3029547, IEEE Transactions on Industry Applications

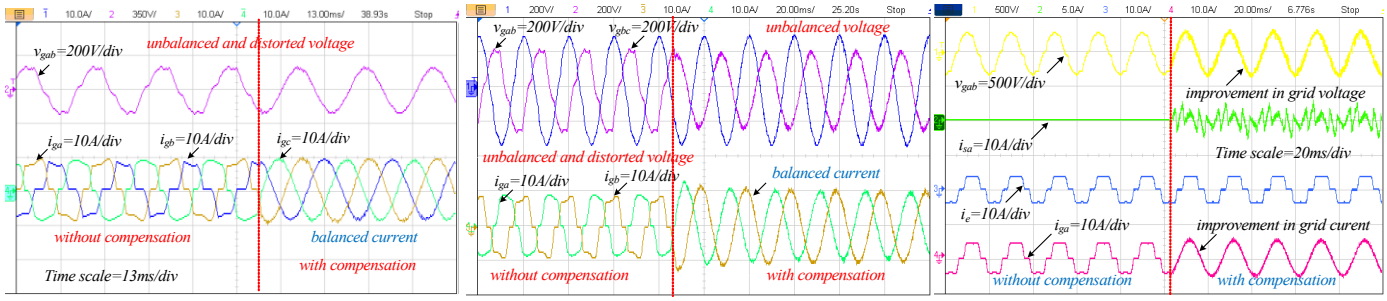

(a) (b) (c)

Fig. 12 Performance at unbalanced and distorted voltage conditions, (a)-(b) grid voltage and grid current, (c) grid voltage and current, load current, and VSC current

verified at different transient conditions caused by the solar irradiance change, wind speed change, home load perturbation, and change in EV current. In addition, the transition from GCM to IM and vice versa and reactive power support to the grid have been successfully presented in detail.

REFERENCES

[1] J. R. Aguero, E. Takayesu, D. Novosel and R. Masiello, "Modernizing the Grid: Challenges and Opportunities for a Sustainable Future," *IEEE Power and Energy Magazine*, vol. 15, no. 3, pp. 74-83, May-June 2017.

[2] International Energy Agency-Global EV Outlook 2020 - Entering the decade of electric drive? [Online]. Available: https://webstore.iea.org/download/direct/3007

[3] S. Wang, S. Bi, Y. A. Zhang and J. Huang, "Electrical Vehicle Charging Station Profit Maximization: Admission, Pricing, and Online Scheduling," *IEEE Trans. Sustain. Energy*, vol. 9, no. 4, pp. 1722-1731, Oct. 2018.

[4] M. K. Gray and W. G. Morsi, "Power Quality Assessment in Distribution Systems Embedded With Plug-In Hybrid and Battery Electric Vehicles," *IEEE Trans. Power Systems*, vol. 30, no. 2, pp. 663-671, March 2015.

[5] M. Falahi, H. Chou, M. Ehsani, L. Xie and K. L. Butler-Purry, "Potential Power Quality Benefits of Electric Vehicles," *IEEE Trans. Sustain. Energy*, vol. 4, no. 4, pp. 1016-1023, Oct. 2013.

[6] S. Jeon, "Discussion of Instantaneous Reactive Power p-q Theory and Power Properties of Three-Phase Systems," *IEEE Trans. Power Delivery*, vol. 23, no. 3, pp. 1694-1695, July 2008.

[7] Kanjiya, B. Singh, A. Chandra, and K. Al-Haddad, "SRF theory revisited" to control self-supported dynamic voltage restorer (DVR) for unbalanced and nonlinear loads," *IEEE Trans. Ind. Appl.*, vol. 49, no. 5, pp. 2330–2340, Sep./Oct. 2013.

[8] F. Wu, L. Zhang and J. Duan, "A New Two-Phase Stationary-Frame-Based Enhanced PLL for Three-Phase Grid Synchronization," *IEEE Trans. Circuits and Systems II: Express Briefs*, vol. 62, no. 3, pp. 251-255, March 2015.

[9] S. Golestan, J. M. Guerrero and J. C. Vasquez, "Single-Phase PLLs: A Review of Recent Advances," *IEEE Trans. Power Electronics*, vol. 32, no. 12, pp. 9013-9030, Dec. 2017.

[10] L. Yang, Y. Chen, A. Luo and K. Huai, "Stability Enhancement for Parallel Grid-Connected Inverters by Improved Notch Filter," *IEEE Access*, vol. 7, pp. 65667-65678, 2019.

[11] R. S. R. Chilipi, N. Al Sayari, K. H. Al Hosani and A. R. Beig, "Adaptive Notch Filter-Based Multipurpose Control Scheme for Grid-Interfaced Three-Phase Four-Wire DG Inverter," *IEEE Trans. Ind. Applicat.*, vol. 53, no. 4, pp. 4015-4027, July-Aug. 2017.

[12] S. Golestan, J. M. Guerrero, F. Musavi and J. C. Vasquez, "Single-Phase Frequency-Locked Loops: A Comprehensive Review," *IEEE Trans. Power Electronics*, vol. 34, no. 12, pp. 11791-11812, Dec. 2019.

[13] S. Golestan, S. Y. Mousazadeh, J. M. Guerrero and J. C. Vasquez, "A Critical Examination of Frequency-Fixed Second-Order Generalized Integrator-Based Phase-Locked Loops," *IEEE Trans. Power Electronics*, vol. 32, no. 9, pp. 6666-6672, Sept. 2017.

[14] F. Xiao, L. Dong, L. Li, and X. Liao, "A frequency-fixed SOGI-based PLL for single-phase grid-connected converters," *IEEE Trans. Power Electron.*, vol. 32, no. 3, pp. 1713–1719, Mar. 2017.

[15] M. A. Akhtar and S. Saha, "An Adaptive Frequency-Fixed Second-Order Generalized Integrator-Quadrature Signal Generator Using Fractional-Order Conformal Mapping Based Approach," *IEEE Trans. Power Electronics*, vol. 35, no. 6, pp. 5548-5552, June 2020.

[16] A. Verma, B. Singh, A. Chandra and K. Al Haddad, "An Implementation of Solar PV Array Based Multifunctional EV Charger," *IEEE Trans. Ind. Applicat*, Early Access.

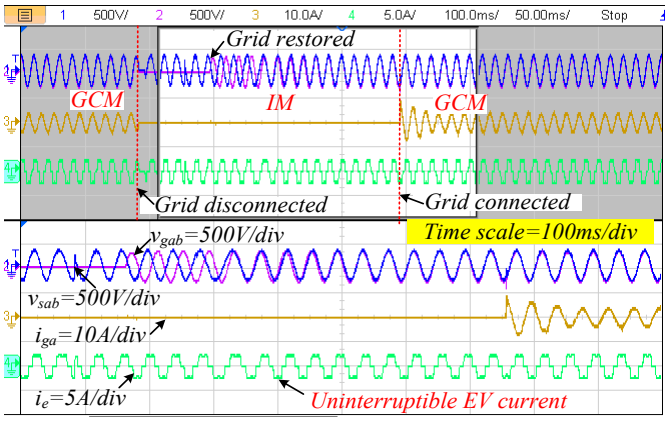

Fig. 13 Synchronization of grid voltage (v_{gab}) and PCC voltage (v_{sab})

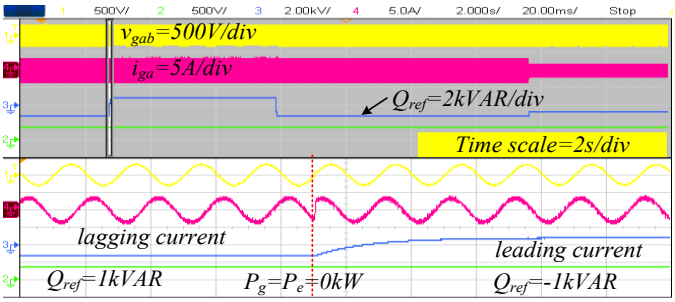

Fig. 14 Reactive power supply to the grid

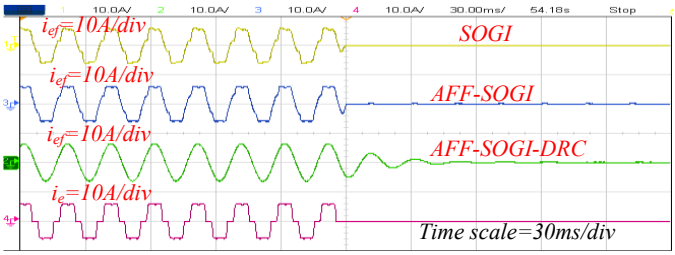

Fig. 15 Comparison of AFF-SOGI-DRC with AFF-SOGI and SOGI algorithms

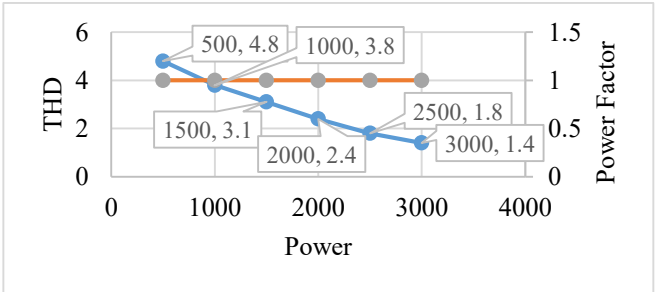

Fig. 16. Grid current THD and power factor with grid power while feeding active power into the grid

[17] S. Singh, P. Chauhan and N. J. Singh, "Feasibility of Grid-Connected Solar-Wind Hybrid System with Electric Vehicle Charging Station," *J. of Modern Power Systems and Clean Energy*, Early Access 2020

[18] F. Elghitani and E. F. El-Saadany, "Efficient Assignment of Electric Vehicles to Charging Stations," *IEEE Trans. Smart Grid*., Early Access 2020.
[19] Y. Deng, Y. Zhang and F. Luo, "Operational Planning of Centralized Charging Stations Using Second-Life Battery Energy Storage Systems," *IEEE Trans. Sustainable Energy*, Early Access 2020.
[20] H. Li, M. A. Azzouz and A. A. Hamad, "Cooperative Voltage Control in MV Distribution Networks with Electric Vehicle Charging Stations and Photovoltaic DGs," *IEEE Syst. J.*, Early Access 2020.
[21] G. R. Chandra Mouli, J. Schijffelen, M. van den Heuvel, M. Kardolus and P. Bauer, "A 10 kW Solar-Powered Bidirectional EV Charger Compatible with Chademo and COMBO," *IEEE Trans, Power Electron.*, vol. 34, no. 2, pp. 1082-1098, Feb. 2019.
[22] T. Alharbi, K. Bhattacharya and M. Kazerani, "Planning and Operation of Isolated Microgrids Based on Re-purposed Electric Vehicle Batteries," *IEEE Trans. Ind. Informat.* Early Access.
[23] A. Verma and B. Singh, "An Implementation of Renewable Energy Based Grid Interactive Charging Station," in *IEEE Transport. Electrification Conf. and Expo (ITEC)*, Detroit, MI, USA, 2019, pp. 1-6.
[24] H. Li, H. Liu, A. Ji, F. Li and Y. Jia, "Design of a hybrid solar-wind powered charging station for electric vehicles," in *IEEE Int. Conf. Materials for Renew. Energy and Env.*. , Chengdu, 2013, pp. 977-981.
[25] A. Verma and B. Singh, "Multi-objective reconfigurable three phase off-board charger for EV," *in IEEE Transport. Electrificat. Conf. (ITEC-India)*, Pune, 2017, pp. 1-6.
[26] D. B. Wickramasinghe Abeywardana, P. Acuna, B. Hredzak, R. P. Aguilera and V. G. Agelidis, "Single-Phase Boost Inverter-Based Electric Vehicle Charger With Integrated Vehicle to Grid Reactive Power Compensation," *IEEE Trans. Power Electron.*, vol. 33, no. 4, pp. 3462-3471, 2018.
[27] Q. Yan, B. Zhang and M. Kezunovic, "Optimized Operational Cost Reduction for an EV Charging Station Integrated with Battery Energy Storage and PV generation," *IEEE Trans. Smart Grid*, Early Access.
[28] K. Chaudhari, A. Ukil, K. N. Kumar, U. Manandhar and S. K. Kollimalla, "Hybrid Optimization for Economic Deployment of ESS in PV-Integrated EV Charging Stations," *IEEE Trans. Ind. Informat*, vol. 14, no. 1, pp. 106-116, Jan. 2018.
[29] V. Monteiro, J. G. Pinto and J. L. Afonso, "Experimental Validation of a Three-Port Integrated Topology to Interface Electric Vehicles and Renewables With the Electrical Grid," *IEEE Trans. Ind. Informat.*, vol. 14, no. 6, pp. 2364-2374, June 2018.
[30] S. Puchalapalli and B. Singh, "A Single Input Variable FLC for DFIG Based WPGS in Standalone Mode," *IEEE Trans. Sustainable Energy*., vol. 11, no. 2, pp. 595-607, April 2020.

Anjeet Verma (M'16) was born in Varanasi (UP), India, in 1991. He received B. Tech. degree in electrical and electronics engineering from G.L. Bajaj Institute of Technology and Management, Gr. Noida (UP), India, in 2012 and the M. Tech. degree in Electrical Machines and Drive from Indian Institute of Technology (BHU), Varanasi (UP) India, in 2015. He is currently working toward the Ph.D. degree in Department of Electrical Engineering from Indian Institute of Technology, Delhi, India. His areas of research interests include electric vehicle, renewable energy based charging infrastructure, power electronics, renewable energy, micro-grid, and power quality.

Bhim Singh (SM'99, F'10) was born in Rahamapur, Bijnor (UP), India, 1956. He received his B.E. (Electrical) from University of Roorkee, India, in 1977 and his M.Tech. (Power Apparatus & Systems) and Ph.D. from Indian Institute of Technology Delhi, India, in 1979 and 1983, respectively. In 1983, he joined Department of Electrical Engineering, University of Roorkee (Now IIT Roorkee), as a Lecturer. In December 1990, he joined Department of Electrical Engineering, IIT Delhi, as an Assistant Professor, where he has become an Associate Professor in 1994 and a Professor in 1997. He has been ABB Chair Professor from September 2007 to September 2012. He has also been CEA Chair Professor from October 2012 to September 2017. He has been Head of the Department of Electrical Engineering at IIT Delhi from July 2014 to August 2016. He has been the Dean, Academics at IIT Delhi from august 2016 to August 2019. He is JC Bose Fellow of DST, Government of India since December 2015. He is the Chairman of BOG of Maulana Azad National Institute of Technology, Bhopal, from 3rd July 2018. He is Non-Official Independent Director, NTPC Limited, from 17th July 2018. He is also Governing Council Member of Central Power Research Institute, Banglore. He has guided 88 Ph.D. Dissertations and 168 M.E./M.Tech. /M.S.(R) theses. He has filed 60 patents. He has executed more than eighty sponsored and consultancy projects. He has co-authored a text book on power quality: Power Quality Problems and Mitigation Techniques published by John Wiley & Sons Ltd. 2015. His areas of interest include solar PV grid systems, microgrids, power quality mitigation, PV water pumping systems, improved power quality AC-DC converters. He is a Fellow of Institute of Engineering and Technology (FIET), Institution of Engineers (India) (FIE), and Institution of Electronics and Telecommunication Engineers (FIETE). He is recipient of JC Bose and Bimal K Bose awards of The Institution of Electronics and Telecommunication Engineers (IETE) for his contribution in the field of Power Electronics. He has received 2017 IEEE PES Nari Hingorani Custom Power Award. He is also a recipient of "Faculty Research Award as a Most Outstanding Researcher" in the field of Engineering-2018 of Careers-360, India. He has received Academic Excellence Award-NPSC-2018. He has also received a Faculty Lifetime Research Award-2018 for overall research contribution at IIT Delhi. He is also a recipient IEEE-IAS Outstanding Educator/Mentor Award 2020, INAE Outstanding Teaching Award 2020 and Eminent Engineer Award-2020 from Institution of Engineers (India).